

# Role of curvature and domain shape on Turing patterns

Sankaran Nampoothiri\* and Amal Medhi†

*School of Physics, Indian Institute of Science Education and Research Thiruvananthapuram, India*

(Dated: May 8, 2017)

We consider pattern formation using reaction-diffusion equation on various non-uniformly curved surfaces. We explore how, in general, curvature and, in particular the domain shape would affect the pattern formation in these geometries. As examples, we study stripe and spot patterns on a torus, and on an ellipsoid. Our results show that the curvature and domain shape can control the orientation of stripe pattern as well as the size and number of spots. Our results also indicate that by controlling the curvature and shape, one can drive the chemicals to a preferred region. Specifically on a torus, curvature and shape can guide the chemicals more on to outer side than inner side. This result may prove important in the studies of self-organization of molecules in biological membranes.

PACS numbers: 87.10.-e, 82.40.Ck, 82.20.-w, 02.40.-k

## I. INTRODUCTION

Pattern formation is an ubiquitous phenomenon in nature. Hence its modeling is of fundamental importance in many fields. After the seminal work of Turing [1], reaction-diffusion systems are widely used for mathematical modeling of spatial pattern formation [2–5]. In reaction-diffusion (RD), chemicals are allowed to react and diffuse so as to produce a patterned steady state. RD equations are routinely used in modeling the skin patterns in fish [6], mammals [7], snakes [8], and leopards [9]. Recently RD equations are also used in understanding the spatial organization of molecules in biological membranes [10]. For example, RD models are proposed to explain oscillations of Min protein system in *E.coli* cells [11–13].

In most studies, RD equations are usually considered on flat geometries for studying patterns. Pattern formation on animal surfaces is an example where the surface is not flat. Another example is the spatial organization of molecules on biological membranes where spherical, saddle and toroidal shaped membranes are common in nature [14, 15]. It is reasonable to assume that curvature and shape of the surface can play an important role in the formation of spatial patterns. For instance, a recent study shows that membrane geometry can control spatial organization of molecules in biological membranes [15]. The geometry can also be responsible for some of the complex patterns observed on animal surfaces [2, 16].

Owing to the importance of geometry on pattern formation, some of the previous studies have considered RD equations on uniformly curved surfaces. For instance, Varea et al. [17] analyzed a generic RD system on a spherical surface, and Zykov et al. [18] studied evolution of spiral waves on the same surface. Meandering of spiral waves on a sphere is thoroughly analyzed using RD equation [19]. RD equation on a hemisphere is used to model the spot formation on the hard wings of lady beetles [20].

Recently, some studies have been initiated to understand RD equations on non-uniformly curved surfaces. To some extent, the role of growth and curvature in RD is attempted in the work of Plaza et al. [21]. The process of parr-marks formation on fish skins are studied where shape of the skin is modeled as growing elliptic cylinder [16]. These studies suggest that the curvature and domain shape can strongly influence the formation of spatial patterns on non-flat geometries. More recently, study on nucleation of RD waves on curved surfaces [22] and spiral waves on curved surfaces [23] again suggest the importance of curvature and domain shape in RD studies.

In this work, we aim to study pattern formation using RD equation on various non-uniformly curved surfaces. In particular, we explore the role of curvature and domain shape in determining the size and the distribution of spot patterns, and orientation of stripe patterns on curved surfaces. We consider RD equation, say, on a torus for different  $R$  and  $r$  values, where  $R$  is major radius and  $r$  is minor radius but keeping the area constant. We then analyze how the number as well as the size and position of the spots and the orientation of stripe patterns vary as we change  $R$  and  $r$ ? Similarly, we also extend our analysis to ellipsoid surface by varying the shape.

The paper is organized as follows. In Sec. II, we give a brief description about the model used for the study. In Sec. III, we study patterns on various non-uniformly curved surfaces, and analyze the role of curvature and domain shape in the formation of patterns on these surfaces. Here we obtain spot and stripe patterns on a torus, and on an ellipsoid. Finally we conclude our results in Sec. IV.

## II. MODEL

The dynamics of RD system on a given curved surface is governed by following set of equations

$$\frac{\partial U}{\partial t} = F_1(U, V) + D_U \Delta_{LB} u, \quad (1a)$$

\* email:sankaran@iisertvm.ac.in

† amedhi@iisertvm.ac.in

$$\frac{\partial V}{\partial t} = F_2(U, V) + D_V \Delta_{LB} v, \quad (1b)$$

where  $U$ ,  $V$  are the concentrations of chemicals,  $F_1(U, V)$ ,  $F_2(U, V)$  represents the reaction kinetics, and  $D_U$ ,  $D_V$  are diffusion coefficients of the chemicals  $U$  and  $V$  respectively, and  $\Delta_{LB}$  is the Laplace-Beltrami operator on curved surface.

Following Barrio et al. [24] we consider specific form of RD equations

$$\begin{aligned} \frac{\partial u}{\partial t} &= \alpha u(1 - r_1 v^2) + v(1 - r_2 u) + D \delta \Delta_{LB} u, \\ \frac{\partial v}{\partial t} &= \beta v(1 + \frac{\alpha r_1}{\beta} uv) + u(\gamma + r_2 v) + \delta \Delta_{LB} v, \end{aligned} \quad (2)$$

where  $u$  and  $v$  are small deviations of  $U$  and  $V$  from homogeneous steady state values. The parameters  $\alpha$ ,  $\beta$ ,  $\gamma$  are related to production and depletion of chemicals. Following Barrio et al., we chose  $\alpha = -\gamma$  in order to have  $(0, 0)$  as the homogeneous steady state. In order to have stable uniform solution, we require either  $\alpha \geq 0$  and  $\beta \leq -\alpha$ , or  $\alpha \leq 0$  and  $\beta \leq -1$ . The ratio of diffusion coefficients between two chemicals is represented by  $D$ , and  $\delta$  scales the system size. Cubic coupling  $r_1$  favors striped patterns while quadratic coupling  $r_2$  favors spot patterns in flat surface and also on a sphere.

The above model was systematically analyzed on two-dimensional flat domain [24]. The model was also thoroughly studied on a sphere to understand the effect of curvature on patterns [17]. Interestingly, these patterns are similar to the patterns of silicate formed on the membranes of Radiolaria.

### III. PATTERN FORMATION ON VARIOUS NON-UNIFORMLY CURVED SURFACES

In this section, we study pattern formation on various non-uniformly curved surfaces. In particular, we analyze the effect of curvature and shape on the formation of patterns in these surfaces. Specifically, we consider formation of spot and stripe patterns on a torus and on an ellipsoid. In order to explore the role of curvature and shape, we obtain patterns on these surfaces by varying the shape parameters (for example,  $R$  and  $r$  on a torus) but keeping the area constant. Our results show that, for the same area, changes in the shape can result in different number of spots, and can also control the orientation of stripe patterns.

#### A. Torus

We now consider the RD equation on a torus and address the following question. How does changes in the  $R$  and  $r$  affect the formation of spatial patterns on a torus? Specifically, we study how the distribution of spots vary as we change the  $R$  and  $r$  of the torus but keeping area constant. In the case of stripe patterns, we analyze how

the orientation depends on the shape of the torus. In order to answer above question, we solve numerically RD equation on a torus for different values of  $R$  and  $r$  keeping the area same in all cases, and thus explore the role of curvature and shape on the formation of spatial patterns.

The surface of a torus can be parametrized as

$$X(\theta, \phi) = \begin{pmatrix} (R + r \cos \theta) \cos \phi \\ (R + r \cos \theta) \sin \phi \\ r \sin \theta \end{pmatrix}, \quad (3)$$

and the coordinates  $\theta$  and  $\phi$  as well as the major radius  $R$  and minor radius  $r$  can be visualized as in Fig. 1. Here both coordinates  $\theta$  and  $\phi$  vary from 0 to  $2\pi$ . The Gauss

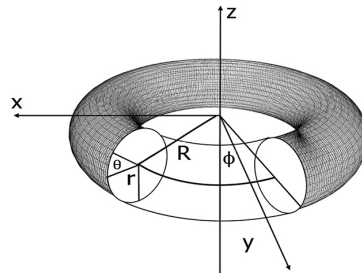


FIG. 1. Schematic representation of the torus parametrized by  $(\theta, \phi)$ .

curvature  $K$  and mean curvature  $H$  of the torus can be read as (see appendix)

$$\begin{aligned} K &= \frac{\cos \theta}{r(R + r \cos \theta)}, \\ H &= \frac{-(2r \cos \theta + R)}{2r(R + r \cos \theta)}, \end{aligned} \quad (4)$$

and note that on a torus both these curvatures are  $\theta$ -dependent. Gauss curvature is positive on the outer side of the torus, and negative on the inner side. Note that the Gauss curvature vanishes at  $\theta = \pi/2$  and  $\theta = 3\pi/2$ . The mean curvature is negative from 0 to  $\pi/2$ , and depending on  $R$  and  $r$ , it can be positive or negative from  $\pi/2$  to  $\pi$ .

In order to solve Eq. (2) numerically on the surface of a torus, we consider the Laplace-Beltrami operator  $\Delta_{LB}$  on the surface of a torus. The Laplace-Beltrami operator is given in curvilinear coordinates as

$$\Delta_{LB} = \sum_{i,j=1}^2 \frac{\partial}{\partial q^i} (\sqrt{g} g^{ij} \frac{\partial}{\partial q^j}), \quad (5)$$

with  $g = \det(g_{ij})$ , where  $g_{ij}$  is the metric elements on the surface. The Laplace-Beltrami operator on a torus is explicitly given by

$$\Delta_{LB} = \frac{1}{(R + r \cos \theta)^2} \frac{\partial^2}{\partial \phi^2} + \frac{1}{r^2} \frac{\partial^2}{\partial \theta^2} - \frac{\sin \theta}{r(R + r \cos \theta)} \frac{\partial}{\partial \theta}, \quad (6)$$

and the Eq. (2) is then numerically solved using the explicit Euler method, where coordinates  $\theta$  and  $\phi$  are discretized as  $\theta_m = m \Delta \theta$ , where  $m = 0, 1, \dots, (M-1)$ , and

$\phi_n = n \Delta \phi$ , where  $n = 0, 1, \dots, (N-1)$ . We use periodic boundary conditions for both  $\theta$  and  $\phi$ . We set the initial condition choosing the random values between -0.5 and 0.5 on a circle near  $\phi = \pi/2$ , and all other points we take  $u = v = 0$ .



FIG. 2. Pattern of  $u$  on a torus with parameters  $D = 0.516$ ,  $\alpha = 0.899$ ,  $\beta = -0.91$ ,  $\gamma = -\alpha$ ,  $\delta = 0.0045$ ,  $r_1 = 3.5$ ,  $r_2 = 0$  with  $R = 1$ ,  $r = 0.1$ .

To begin with, the pattern on a torus with parameters specified in the caption of Fig. 2 is obtained with  $2\pi r < \lambda_T$ , where  $\lambda_T$  is the Turing length. Since  $2\pi r < \lambda_T$ , the above case is similar to pattern formation on a cylinder with radius  $r$  and height  $2\pi R$ . As expected we obtain 10 rings on the torus. In this case taking different  $R$  and  $r$  values with  $2\pi r < \lambda_T$  only changes the number of rings on the torus. Here the ring-like shape of the pattern will not change as we vary  $R$  and  $r$ . Thus the shape of the torus will not produce any qualitative changes on patterns when  $2\pi r < \lambda_T$ . In order to see the effect of curvature and domain shape on patterns, we consider  $2\pi r > \lambda_T$ , and then produce different patterns on a torus by changing  $R$  and  $r$  values.

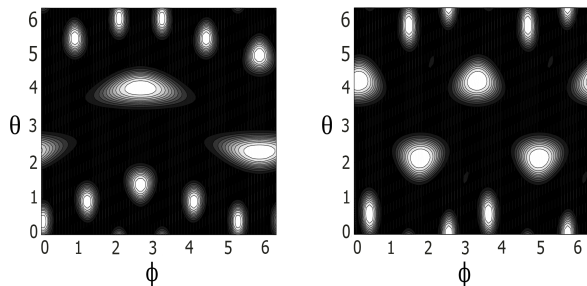


FIG. 3. Left is the 12 spots on a torus with  $R = 0.6$ ,  $r = 1/0.6\pi$  and right is the 10 spots with  $R = 0.7$ ,  $r = 1/0.7\pi$ . The parameter values are  $D = 0.516$ ,  $\alpha = 0.899$ ,  $\beta = -0.91$ ,  $\gamma = -\alpha$ ,  $\delta = 0.0085$ ,  $r_1 = 0.02$ ,  $r_2 = 0.2$ . Vertical axis is  $\theta$  and  $\phi$  is horizontal axis.

First we consider formation of spot patterns on the torus. We choose the parameter values  $r_1 = 0.02$ ,  $r_2 = 0.2$ , which result in spot patterns on flat surface, and on sphere. We obtain patterns with 12 spots and 10 spots on a torus, as shown in Fig. 3, for two cases respectively both with same area and initial condition but

with different values of shape parameter. This result thus shows that the number of spots can be influenced by the shape. Here, the torus with smaller  $R$  has more number of spots compared to the torus with large  $R$ . Note that in both cases number of spots are more in the region  $0 < \theta < \pi/2$  compared to the region  $\pi/2 < \theta < \pi$ .

We also observe that the number of spots in region  $0 < \theta < \pi/2$  is more in the case of a torus with smaller  $R$ . Specifically, torus with smaller  $R$  has 7 spots in this region but the torus with higher  $R$  contain only 6 spots. But in the region between  $\pi/2$  and  $\pi$  the torus with smaller  $R$  has one spot, and the torus with larger  $R$  contain two spots. The size of the spots are larger in the region between  $\pi/2$  and  $3\pi/2$  in both cases of higher and smaller  $R$ . Note that the smaller  $R$  has larger spots in this region compared to higher  $R$ .

In both cases, outer side of the torus contain more number of spots than inner side. These results thus illustrate that specific values of shape parameters can result in localization of chemicals, where the concentration can be more on outer side of the torus than inner side. Note that the quadratic term  $r_2$  favors spot patterns on the surface of a torus like in flat and spherical geometry.



FIG. 4. Stripe pattern on a torus with parameters  $D = 0.516$ ,  $\alpha = 0.899$ ,  $\beta = -0.91$ ,  $\gamma = -\alpha$ ,  $\delta = 0.0045$ ,  $r_1 = 3.5$ ,  $r_2 = 0$  with  $R = 1$ ,  $r = 0.3$ .

Next we study stripe patterns on a torus. We obtain different orientation of stripe patterns by changing  $R$  and  $r$  as shown in Fig. 4 and Fig. 5. In the first case, we produce stripe pattern wrapping around the torus. In the second case, with same initial condition and parameters as in the first case, we obtain ring-like pattern where the concentration is varying only along  $\theta$ -direction by changing  $R$  and  $r$ . Thus changes in the shape can result in different orientation of stripe patterns on toroidal surfaces. Note that the cubic term  $r_2$  favors stripe patterns on the surface of a torus like in the flat and the spherical geometry.

An intuitive understanding of our results can be given in the following way. As described in [22], the Laplace-Beltrami operator  $\Delta_{LB}$  on a torus can be mapped to as Laplace operator on a flat surface with a

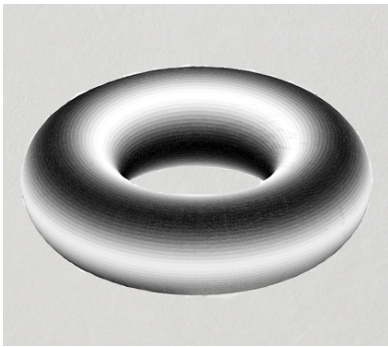


FIG. 5. Stripe pattern on a torus with parameters  $D = 0.516$ ,  $\alpha = 0.899$ ,  $\beta = -0.91$ ,  $\gamma = -\alpha$ ,  $\delta = 0.0045$ ,  $r_1 = 3.5$ ,  $r_2 = 0$  with  $R = 0.90946$ ,  $r = 0.35$ .

conformal factor, and is given as

$$\Delta_{LB} = \frac{(\cosh \eta - \cos \theta_i)^2}{a^2} \left( \frac{\partial^2}{\partial \theta_i^2} + \frac{\partial^2}{\partial \phi^2} \right), \quad (7)$$

where

$$\begin{aligned} a &= (R^2 - r^2)^{1/2}, \\ \eta &= \coth^{-1} \left( \frac{R}{\sqrt{R^2 - r^2}} \right), \\ \tilde{\phi} &= \phi \sinh \eta, \\ \cos \theta_i &= \cosh \left[ \coth^{-1} \left( \frac{R}{\sqrt{R^2 - r^2}} \right) \right] - \frac{a \sinh \frac{R}{\sqrt{R^2 - r^2}}}{r \cos \theta + R}. \end{aligned}$$

Thus the RD equation on a torus can be equivalently described as a RD equation on a flat surface where  $\delta$  is replaced by  $\theta$ -dependent  $\delta_{eff}$ , where  $\delta_{eff} = \delta(\cosh \eta - \cos \theta_i)^2/a^2$ . Hence, the effect of curvature is equivalent to having a spatially varying parameter  $\delta_{eff}$ . Since the variations in the  $\delta_{eff}$  depends on  $R$  and  $r$ , the orientation of stripe pattern as well as the size and number of spots can vary as we change the shape of the torus.

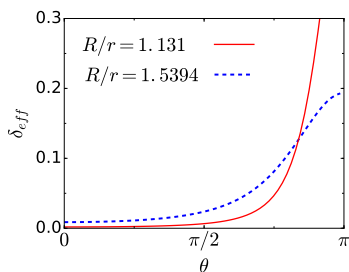


FIG. 6. Figure illustrates the variation of  $\delta_{eff}$  as the coordinate  $\theta$  changes.

Here we illustrate the effect of local variation in  $\delta$  by considering the example of RD on a cylinder. We consider the RD equation on a cylinder with parameters as specified in the caption Fig. 4, with radius  $r = 0.3$  and

height  $h = 2\pi$ . In this case, we have obtained an inhomogeneous concentration along  $\theta$ -direction on a cylinder, but stripe pattern will not wrap around the cylinder. The stripe pattern on the cylinder thus clearly differs from the stripe pattern that wraps on the torus with same initial condition. Now suppose we assume two different values in the parameter  $\delta$  on a cylinder, where  $\delta = 0.0085$  for  $0 \leq \theta \leq (M/2 - 1)2\pi/M$  and  $\delta = 0.0045$  for  $\pi \leq \theta \leq (M - 1)2\pi/M$ , and with same initial condition as above. In this case we obtain a stripe pattern with varying concentration along the of  $\theta$ -direction, where the stripe wraps around the cylinder. This example thus illustrate that the wrapping of stripe pattern on a torus is due to curvature, and whose effect is equivalent to having a spatial-dependent  $\delta_{eff}$ , and not due to a specific initial condition.

Suppose we now change  $\delta$ , say to 0.0085 for  $0 \leq \theta \leq (M/2 - 1)2\pi/M$  and to 0.011559 for  $\pi \leq \theta \leq (M - 1)2\pi/M$ . Then we obtain the pattern on a cylinder which is qualitatively same as the pattern obtained on the second torus in the Fig. 5, where it forms a ring-like pattern with variation along  $\theta$ -direction. Thus, different local variations in  $\delta$  can give different orientations to the stripe pattern. Thus the changes in the shape can give different spatial variations in  $\delta$ , which in turn can lead to different orientation of stripe patterns.

The localization of chemicals in preferred regions and an increase in the size of the spots in certain regions can also be intuitively understood in the following way. Note from the Fig. 6, the  $\delta_{eff}$  increases from  $\theta = 0$  to  $\pi$ , but the gradient in  $\delta_{eff}$  is large in the region  $\pi/2$  to  $\pi$ . Since the Turing wavelength increases with increase in  $\delta$ , in this picture one can intuitively argue that an increase in  $\delta_{eff}$  can lead to higher wavelength mode in the region  $\pi/2$  to  $\pi$  compared to  $\theta = 0$  to  $\pi/2$ . Since the gradient in  $\delta_{eff}$  is large and positive in the region  $\pi/2$  to  $\pi$  on a torus with both smaller and larger  $R$ , one can expect less number of spots with larger size in the region  $\pi/2$  to  $\pi$  compared to that between 0 to  $\pi/2$  in both cases. Note that the large gradient in  $\delta_{eff}$  can result in the localization of chemicals and larger size spots in some preferred regions.

To sum up, varying  $R$  and  $r$  on the torus can lead to different  $\delta_{eff}$  which in turn can control the size and distribution of spots, and can also lead to different orientation of stripes. Our results also indicate that by controlling the curvature and shape one can drive the chemicals to a preferred region. This result may useful in the studies of self-organization of molecules in biological membranes.

## B. Ellipsoid

We now consider the pattern formation on an ellipsoid. Specifically, we obtain patterns on oblate and prolate spheroid with same area, and analyze the role of curvature and shape parameters on the number of spots,

and on the orientation of stripe pattern. The equation of an ellipsoid is

$$\frac{x^2 + y^2}{a^2} + \frac{z^2}{b^2} = 1, \quad (8)$$

where the case with  $a > b$  is called oblate spheroid, while the case with  $a < b$  is prolate spheroid. The ellipsoid can be parametrized as

$$X(\theta, \phi) = \begin{pmatrix} a \sin \theta \cos \phi \\ a \sin \theta \sin \phi \\ b \cos \theta \end{pmatrix}, \quad (9)$$

where  $\theta$  and  $\phi$  are the coordinates on the surface. Note that on an ellipsoid both curvatures are  $\theta$ -dependent. The Gaussian curvature of an ellipsoid is positive (see appendix) where the curvature varies from  $b^2/a^4$  (at  $\theta = 0$ ) to  $1/b^2$  (at  $\theta = \pi/2$ ).

We solve Eq. (2) numerically on the surface of an ellipsoid. The Laplace-Beltrami operator  $\Delta_{LB}$  on an ellipsoid can be read from  $g_{ij}$  (see appendix) and given as

$$\Delta_{LB} = \frac{1}{(a^2 \cos^2 \theta + b^2 \sin^2 \theta)} \frac{\partial^2}{\partial \theta^2} + \frac{1}{a^2 \sin^2 \theta} \frac{\partial^2}{\partial \phi^2} + \left( \frac{\cot \theta}{(a^2 \cos^2 \theta + b^2 \sin^2 \theta)} + \frac{(1 - b^2/a^2) \sin 2\theta}{2a^2(\cos^2 \theta + b^2/a^2 \sin^2 \theta)^2} \right) \frac{\partial}{\partial \theta},$$

and the co-ordinates on an ellipsoid can be discretized as  $\theta_m = (m + 1/2) \Delta \theta$ , where  $m = 0, 1, \dots, (M - 1)$ , and  $\phi_n = n \Delta \phi$ , where  $n = 0, 1, \dots, (N - 1)$ . Following [17], we consider the nearest neighbor of  $u(m = 0, M; n = 0, 1, \dots, N/2 - 1)$  is  $u(m = 0, M; N/2, \dots, N - 1)$ , and for  $\phi$  co-ordinate we use periodic boundary condition. The same condition is taken for  $v$  also. We choose initial condition as random values between -0.5 and 0.5 on a circle near equator, and all other points we take  $u = v = 0$ .

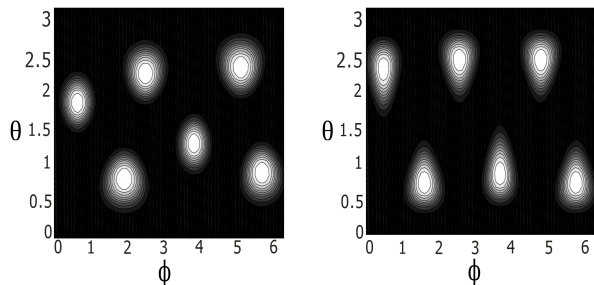


FIG. 7. Left is the 6 spots on a prolate spheroid with  $b = 1.1$ ,  $a = 0.9$  and right is the 6 spots on an oblate spheroid of same area with  $b = 0.50493$ ,  $a = 1.2$ . The parameter values are  $D = 0.516$ ,  $\alpha = 0.899$ ,  $\beta = -0.91$ ,  $\gamma = -\alpha$ ,  $\delta = 0.0171$ ,  $r_1 = 0.02$ ,  $r_2 = 0.2$ .

First we consider formation of spot patterns. We obtain 6 spots on an oblate spheroid and 6 spots on prolate spheroid with same initial condition and area but with

different values of  $b$  and  $a$  as shown in Fig. 7. Note that the position of spots are different in both cases. Thus it is clear that the elongation of an ellipsoid can control the position of spot patterns. Furthermore, numerical simulations give 6 spots when  $b = 0.99$ ,  $a = 1$  as shown in Fig. 8. This is exactly same as the previous result obtained on a sphere [17] with same parameters. The above result illustrates that small deviations from uniform curvature cannot influence pattern formation as pointed out in [16].

It is interesting to note that position and number of spots on a prolate spheroid with  $b = 1.1$  and  $a = 0.9$  is exactly same as that on a sphere with  $b = 1$  and  $a = 1$ . But the position of spots on the oblate spheroid is different from that on a sphere. Here, the effect of curvature and shape is more pronounced in the case of an oblate spheroid compared to the prolate one. Note that the quadratic term  $r_2$  favors spot patterns on the surface of an ellipsoid like in the other geometries considered.

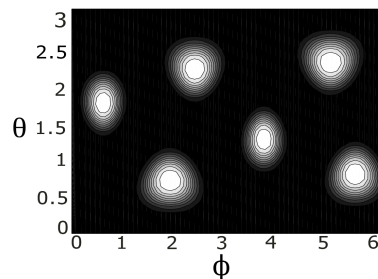


FIG. 8. 6 spot pattern with  $b = 0.99$ ,  $a = 1$ . Other parameters are same as in Fig. 7.

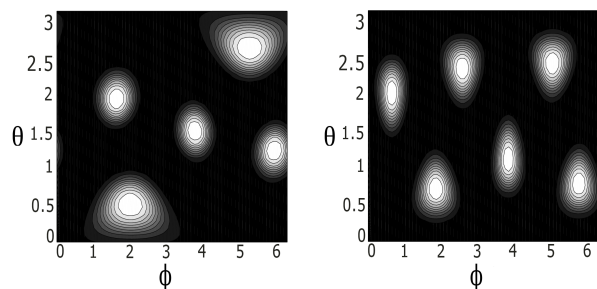


FIG. 9. Left is the 5 spots on a prolate spheroid with  $b = 1.10409$ ,  $a = 0.8$  and right is the 6 spots on an oblate spheroid of same area with  $b = 0.7$ ,  $a = 1$ . The parameter values are  $D = 0.516$ ,  $\alpha = 0.899$ ,  $\beta = -0.91$ ,  $\gamma = -\alpha$ ,  $\delta = 0.0171$ ,  $r_1 = 0.02$ ,  $r_2 = 0.2$ .

As shown in the Fig. 9, we again produce spots where the parameters considered are same as in the caption of Fig. 7, but with different shape. We have then obtained different number of spots on a prolate and an oblate spheroid. Specifically oblate spheroid has more number of spots compared to the prolate one. In this case, note that the size of spots below  $\theta = \pi/4$  and above  $\theta = 3\pi/4$

are larger on the prolate spheroid. Thus the effects of the curvature and domain shapes are more pronounced in this case compared to the previous one given in the Fig. 7.

Next we consider the formation of stripe patterns. Fig. 10 shows stripe patterns on a prolate spheroid and an oblate spheroid of same surface area. Note that the orientation of stripe patterns are different in both cases. Hence the elongation of an ellipsoid can influence the orientation of stripe patterns. Similar to other geometries considered earlier, even in the case of ellipsoid the cubic term  $r_1$  favors stripe patterns.

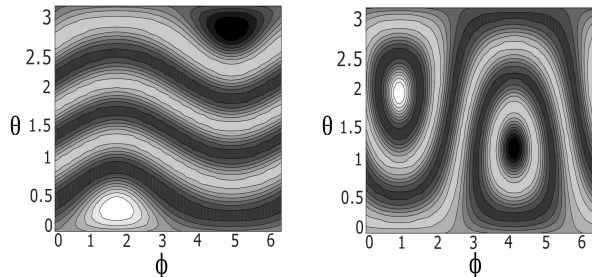


FIG. 10. Left is the stripe pattern on a prolate spheroid with  $b = 1.2, a = 1$  and right is on an oblate spheroid  $b = 1, a = 1.09884$ . The parameter values are  $D = 0.516, \alpha = 0.899, \beta = -0.91, \gamma = -\alpha, \delta = 0.0085, r_1 = 0.02, r_2 = 0$ .

#### IV. CONCLUSION

To sum up, we have studied pattern formation on various non-uniformly curved surfaces. In particular, we analyzed the role of curvature and shape on the pattern formation. First we obtained spot and stripe patterns on a torus. To begin with, we have produced patterns on a torus similar to that on a cylinder by considering  $2\pi r < \lambda_T$ . We have then relaxed the above condition, and obtained spot and stripe patterns for different  $R$  and  $r$  values. For the same area, our results indicate that the orientation of stripe pattern as well as the size and number of spots can be controlled by the shape of the torus.

Our analysis on a torus shows that the number of spots can be controlled by the major and minor radii  $R$  and  $r$  of the torus, respectively. Secondly the curvature and domain shape can also control the size of the spots. For the parameter values considered, the number of spots on the outer side of the torus in each case is found to be more than that on the inner side, the difference in number being dependent on the gradient in the parameter  $\delta_{eff}$ . We also show that it is possible to produce different orientations of stripe patterns by changing  $R$  and  $r$ . Thus our results indicate that curvature and shape can play an important role in the formation of patterns on non-flat geometries.

We have also suggested an intuitive way of understanding the effect of curvature and shape. On a torus, the effect of curvature is equivalent to replacing the parameter  $\delta$  by a space-dependent parameter  $\delta_{eff}$ . The parameter  $\delta_{eff}$  can vary only along  $\theta$ - direction and depends on the shape parameters. Thus the shape can control the formation of patterns. Note that from the  $\delta_{eff}$  one can identify outer side of the torus can have more number of spots compared to inner side. The conformal factor also can be useful to understand the size of the spots in different regions. Hence calculating conformal factor either analytically or numerically on various curved surfaces can be important in RD studies.

We then studied spot and stripe patterns on both prolate and oblate spheroid. We show that the number and position of spot patterns can depend on the elongation of an ellipsoid. In one case, we have obtained less number of spots on a prolate spheroid, while in other case both prolate and oblate spheroid contains same number of spots. Our analysis shows that shape parameters can influence both position as well as the size and number of spots on an ellipsoid similar to that on a torus. We also showed that the difference in shape (oblate or prolate spheroid) can result in different orientation of stripe patterns.

It is clear from our analysis that the curvature effect is equivalent to having an effective anisotropy in local parameters that can lead to new effects on patterns that it is different from flat case. The effect of anisotropy in local parameters is studied in some of the previous works [25, 26]. For instance, effect of anisotropy in diffusion coefficient on flat surface is analyzed [26], and showed that the resulting pattern can have spatially varying amplitude and wavelength. This is similar to our observations, for example, on a torus where the distance between the spots and their size vary with position. Similarly, features like stratification of labyrinthine patterns due to anisotropic diffusion mentioned in the work [25] can also arise in RD systems on curved surfaces.

Some of the earlier studies explained the directionality of stripe patterns on fishes by introducing anisotropic diffusion coefficients in RD equations on a flat surface [6, 27]. Since the curvature can control the orientation of stripe pattern, it would be imperative to incorporate the effect of curvature in understanding the directionality of stripe patterns on fishes. Turing-like patterns are observed in microorganisms with elongated structure like Radiolaria. Analysis similar to that adapted here may be suitable to study and mimic the patterns on such viruses. Moreover, since RD models are being used to understand the self-organization of molecules on biological membranes, where toroidal and ellipsoid shapes are common, the above analysis thus may be useful to understand the curvature effects on self-organization in such membranes. It would be also interesting to extend our analysis to other geometries, such as hyperboloid surface which seems to play an important role in biological materials [28].

## V. ACKNOWLEDGEMENT

We acknowledge Sreedhar Dutta for suggesting the problem, and for useful discussions. We also thank him for various helpful comments during the preparation of the manuscript.

### Appendix A: Geometric quantities on a torus and on an ellipsoid

The torus can be parametrized as

$$X(\theta, \phi) = \begin{pmatrix} (R + r \cos \theta) \cos \phi \\ (R + r \cos \theta) \sin \phi \\ r \sin \theta \end{pmatrix},$$

and using the above parametrization one can read intrinsic and extrinsic quantities related to curvature as

$$g_{\theta\theta} = r^2, \quad g_{\phi\phi} = (R + r \cos \theta)^2, \quad g_{\theta\phi} = g_{\phi\theta} = 0, \\ \kappa_{\theta\theta} = -r, \quad \kappa_{\phi\phi} = -(R + r \cos \theta) \cos \theta, \quad \kappa_{\theta\phi} = \kappa_{\phi\theta} = 0,$$

and then using the intrinsic and extrinsic quantities, the gauss curvature  $K$  and mean curvature  $H$  on a torus can be read as

$$K = \frac{\cos \theta}{r(R + r \cos \theta)},$$

$$H = \frac{-(2r \cos \theta + R)}{2r(R + r \cos \theta)}.$$

The ellipsoid can be parametrized as

$$X(\theta, \phi) = \begin{pmatrix} a \sin \theta \cos \phi \\ a \sin \theta \sin \phi \\ b \cos \theta \end{pmatrix},$$

and using the above parametrization we read intrinsic and extrinsic quantities related to curvature as

$$g_{\theta\theta} = a^2(\cos^2 \theta + \frac{b^2}{a^2} \sin^2 \theta), \quad g_{\phi\phi} = a^2 \sin^2 \theta, \quad g_{\theta\phi} = g_{\phi\theta} = 0, \\ \kappa_{\theta\theta} = \frac{b}{(\cos^2 \theta + \frac{b^2}{a^2} \sin^2 \theta)^{1/2}}, \quad \kappa_{\phi\phi} = \frac{b \sin^2 \theta}{(\cos^2 \theta + \frac{b^2}{a^2} \sin^2 \theta)^{1/2}}, \\ \kappa_{\theta\phi} = \kappa_{\phi\theta} = 0,$$

and then gauss and mean curvature on an ellipsoid is given by

$$K = \frac{b^2}{a^4(\cos^2 \theta + \frac{b^2}{a^2} \sin^2 \theta)^2}, \\ H = b \frac{1 + (\cos^2 \theta + \frac{b^2}{a^2} \sin^2 \theta)}{2a^2(\cos^2 \theta + \frac{b^2}{a^2} \sin^2 \theta)^{3/2}}.$$

- 
- [1] A. M. Turing, Philosophical Transactions of the Royal Society of London B: Biological Sciences **237**, 37 (1952).
  - [2] J. D. Murray, *Mathematical Biology. II Spatial Models and Biomedical Applications* {*Interdisciplinary Applied Mathematics V. 18*} (Springer-Verlag New York Incorporated, 2001).
  - [3] A. Koch and H. Meinhardt, Reviews of modern physics **66**, 1481 (1994).
  - [4] F. Borgogno, P. D'Odorico, F. Laio, and L. Ridolfi, Reviews of Geophysics **47** (2009).
  - [5] S. Getzin, H. Yizhaq, B. Bell, T. E. Erickson, A. C. Postle, I. Ktra, O. Tzuk, Y. R. Zelnik, K. Wiegand, T. Wiegand, *et al.*, Proceedings of the National Academy of Sciences **113**, 3551 (2016).
  - [6] H. Shoji, Y. Iwasa, A. Mochizuki, and S. Kondo, Journal of Theoretical Biology **214**, 549 (2002).
  - [7] J. B. Bard, Journal of Theoretical Biology **93**, 363 (1981).
  - [8] J. D. Murray and M. Myerscough, Journal of theoretical biology **149**, 339 (1991).
  - [9] R. Liu, S. Liaw, and P. Maini, Physical review E **74**, 011914 (2006).
  - [10] M. Loose, K. Kruse, and P. Schwill, Annual review of biophysics **40**, 315 (2011).
  - [11] M. Howard, A. D. Rutenberg, and S. de Vet, Physical review letters **87**, 278102 (2001).
  - [12] G. Meacci and K. Kruse, Physical biology **2**, 89 (2005).
  - [13] H. Meinhardt and P. A. de Boer, Proceedings of the National Academy of Sciences **98**, 14202 (2001).
  - [14] H. T. McMahon and J. L. Gallop, Nature **438**, 590 (2005).
  - [15] R. Parthasarathy and J. T. Groves, Soft Matter **3**, 24 (2006).
  - [16] C. Venkataraman, T. Sekimura, E. A. Gaffney, P. K. Maini, and A. Madzvamuse, Physical Review E **84**, 041923 (2011).
  - [17] C. Varea, J. Aragon, and R. Barrio, Physical Review E **60**, 4588 (1999).
  - [18] V. Zykov, A. Mikhailov, and S. Müller, Physical review letters **78**, 3398 (1997).
  - [19] J. Gomata and F. Amdjadi, Physical Review E **56**, 3913 (1997).
  - [20] S. Liaw, C.-C. Yang, R. Liu, and J. Hong, Physical Review E **64**, 041909 (2001).
  - [21] R. G. Plaza, F. Sanchez-Garduno, P. Padilla, R. A. Barrio, and P. K. Maini, Journal of Dynamics and Differential Equations **16**, 1093 (2004).
  - [22] F. Kneer, E. Schöll, and M. A. Dahlem, New Journal of Physics **16**, 053010 (2014).
  - [23] H. Dierckx, E. Brisard, H. Verschelde, and A. V. Panfilov, Physical Review E **88**, 012908 (2013).
  - [24] R. Barrio, C. Varea, J. Aragón, and P. Maini, Bulletin of mathematical biology **61**, 483 (1999).
  - [25] M. Bär, E. Meron, and C. Uetzny, Chaos: An Interdisciplinary Journal of Nonlinear Science **12**, 204 (2002).
  - [26] D. Benson, P. Maini, and J. Sherratt, Mathematical and computer modelling **17**, 29 (1993).
  - [27] H. Shoji, A. Mochizuki, Y. Iwasa, M. Hirata, T. Watanabe, S. Hioki, and S. Kondo, Developmental dynamics **226**, 627 (2003).

- [28] M. E. Evans and G. E. Schröder-Turk, *Asia Pacific Mathematics Newsletter* **5**, 21 (2015).